OE Optical Engineering

RESEARCH PAPER

Speckle control for electro-holographic display using high-brightness yellow phosphor light source in projector

Takuo Yoneyama* **and Yuji Sakamoto**
Hokkaido University, Graduate School of Information Science and Technology, Sapporo, Japan

ABSTRACT. In electronic holography, a light source that can control coherence steplessly is desired to adjust the balance between speckle noise and the resolution of reconstructed images. We propose a high-brightness light source that can control speckle by adjusting the bandwidth. In general, narrowing the bandwidth of the light source results in a decrease in brightness. To compensate for this, the proposed system contains a yellow phosphor light source in the projector as a high-intensity light source. The results of experiments show that bandwidth of the proposed device can be adjusted as intended, and it is brighter than high brightness light emitting diode. Therefore, it is confirmed that the proposed device is useful as a reconstruction light source for electro-holography with evaluating the quality of reconstructed images.

Keywords: electro-holography; high power light source; controllable bandwidth light source; speckle noise

Paper 20230389G received Apr. 25, 2023; revised Jul. 23, 2023; accepted Aug. 10, 2023; published Aug. 25, 2023; corrected Aug. 26, 2023.

1 Introduction

Laser diodes (LDs) are used in various image display devices such as laser displays and projectors due to their properties such as high color purity and high coherence. However, it is known that visual noise called speckle noise occurs in image display devices that use coherent light sources, regardless of the intended image, and significantly impairs the quality of reconstructed images.[1] This is the same problem with computer-generated holograms (CGHs), which are considered an ideal 3D imaging display technology, and is a major obstacle for the practical use of CGH. Therefore, many studies have been conducted on the suppression of speckle noise.[2–11] Laser speckle noise reduction methods can be broadly divided into hardware and software approaches. In the hardware approach, the aim is to change the hardware and optical system without changing the conventional hologram data. In contrast, the software approach does not change the hardware and generates hologram data with less speckle noise.

Proposed software approaches include converging the object light at the observation point without random phase when calculating CGHs[2] and the Gerchberg–Saxton algorithm for phase-only holograms.[3] Although these methods generate hologram data with reduced speckle noise, the drawback is that they cannot be combined with other calculation algorithms and require a long calculation time. Other methods are based on time-division multiplexing,[4–7] where the reconstructed image is divided into several parts, which are then displayed sequentially. These methods required a display device with high frame rate when applying sequential colorization or animation for averaging by time-division multiplexing.

*Address all correspondence to Takuo Yoneyama, yoneyama@eis.hokudai.ac.jp

Therefore, in our study, we focus on the hardware-based speckle suppression approach because of its versatility; for example, there is no need to change the data and there are no restrictions imposed by the performance of the display device. Hardware approaches include angle multiplexing by laser scanning using a micromirror,[8] transmission through a vibrating diffusion plate using a dielectric elastomer,[9] and transmission through vibration using a tuning fork[10] or rotating frosted glass.[11] The reconstruction light source can be replaced with the proposed light source without recalculating hologram data.

Most hardware speckle suppression techniques reduce the coherence of the light source in some way. However, in general, when the coherence of the light source is lowered, the speckle noise is suppressed but the resolution of the CGH reconstruction image is also lowered in the process.[12] Therefore, to improve the overall image quality, the coherence of the light source must be adjusted to a well-balanced value that does not impair the sense of resolution of the reconstructed image or make it difficult to visually recognize speckles.

As explained in Sec. 2.1, coherence is divided into spatial and temporal. Approaches to reducing spatial coherence include using a moving diffuser[8–11] and vibrating an optical fiber.[13] Meanwhile, approaches to reducing temporal coherence include using multiple lasers with different central wavelengths[14] and using a broadband light source.[12,15] The previous studies[12,15] compared speckle noise when using light sources with different bandwidths, such as LD, light emitting diode (LED), and superluminescent LED. However, because a light source device capable of steplessly controlling coherence was not used, the coherence value that optimizes the balance between speckle and resolution could not be experimentally determined. In other words, due to the low flexibility of full width at half maximum (FWHM), the above-mentioned balanced coherence optimum could not be reached in the previous studies.[12,15]

We propose a novel reconstruction light source of electro-holography that is bright and can freely adjust temporal coherence by steplessly controlling the bandwidth. A yellow phosphor light emitted from the projector is used as a high-brightness broadband light source. Using variable bandwidth bandpass filter (BPF) with adjusting the bandwidth, the temporal coherence of the light can be controlled. In this paper, we report the basic operation and effectiveness of the proposed device determined from CGH reconstruction experiments.

2 Coherence and Quality of Reconstructed Image

2.1 Speckle Noise

There are two types of optical coherence, spatial coherence and temporal coherence. Spatial coherence is the degree of order between light waves at different points in space. In contrast, the temporal coherence of light is the degree of order between lights emitted from the same point at different times. The temporal coherence is maximum when the emitted light contains a single wavelength, and it becomes lower as more light of different wavelengths is contained. In other words, the wider the wavelength band, the lower the coherence.

Figure 1 shows a schematic diagram of the principle when speckles are visually recognized. Speckle noise is random spotty visual noise observed when spatially and temporally coherent

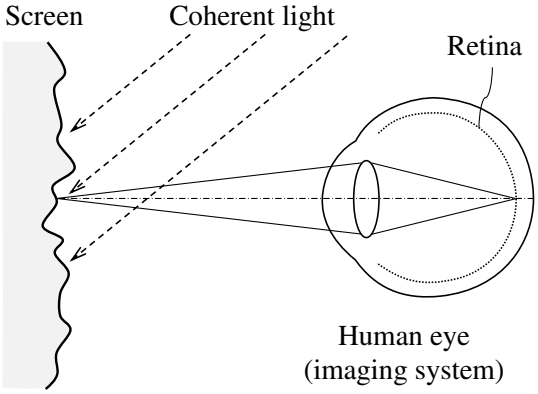

Fig. 1 Schematic diagram of human eye recognizing speckle.

light such as LD light is scattered on a rough surface.[16] The interference pattern formed on the retina deforms along with the wavefront of the light incident on the retina, so when the angle of incident light changes due to the change in pupil diameter, the visible speckle pattern also deforms.

When quantitatively evaluating speckle, speckle contrast C_s is used as an index to indicate speckle intensity, as represented by the following equation:

$$C_s = \frac{\sigma_n}{\langle I \rangle}, \tag{1}$$

where σ_n and $\langle I \rangle$ are the standard deviation and the mean intensity of the reconstructed image, respectively. C_s is 1.0 when the illumination light is complete coherent light and an object consists of perfectly diffusing surfaces, which is referred to as fully developed speckle. $C_s = 0$ indicates that there is no speckle noise. The relationship between C_s and the bandwidth W is expressed by the following equation:[17]

$$C_s \propto \frac{1}{\sqrt[4]{1 + (2W\sigma)^2}}, \tag{2}$$

where W is the bandwidth of the illumination light, and σ is the surface roughness. Here, if $1 \ll W_\sigma$ in Eq. (2), the ratio of the speckle contrast C, C' to the illumination light with bandwidth W, W' on the surface of the same roughness can be expressed as

$$\frac{C'}{C} \propto \sqrt{\frac{W\sigma}{W'\sigma'}}. \tag{3}$$

In this case, the speckle contrast ratio and the bandwidth ratio are inversely proportional. Therefore, if the bandwidth is adjusted steplessly, the speckle contrast can be freely controlled.

2.2 Effect of Coherence on CGH Reconstructed Image

In holography, there is a close relationship between the resolution of the reconstructed image and the coherence of the light source.[12] In general, hologram cannot image a bright spot smaller than the emission size of the light source due to the diffraction limit. Therefore, reducing the emission size and increasing the spatial coherence are directly linked to improving the resolution of the reconstructed image. In addition, CGH is calculated for a specific wavelength, and it is assumed that the reconstruction light has the same wavelength.

Considering the case where the CGH calculated at a specific wavelength is reconstructed at a slightly different wavelength, an image is formed at a position that deviates from the target spatial coordinates accordingly. When a light source has wavelengths with a wide bandwidth, the convergence of points with different spatial image forming positions continuously causes a blurring effect, which reduces the sense of resolution. In other words, the more the temporal coherence increases, the more this blurring effect is eliminated, and as a result, the resolution of the reconstructed image is improved.

The sense of resolution of the reconstructed image is improved using spatially and temporally coherent light. However, as described in the previous section, light with high coherence forms strong speckles, so a higher coherence does not necessarily mean that the light source is more suitable for holographic reconstruction. Therefore, to ensure the quality of the reconstructed image, the light source should be well balanced such that it ensures a certain degree of coherence for the sense of resolution while reducing the visibility of speckles.

2.3 *Laser Phosphor Light Source*

In general, LDs, which are spatially and temporally coherent light sources, are widely used for the reconstruction of electro-holography. However, because of the high coherence of LDs, speckle noise can significantly degrade image quality, so high-brightness LEDs are often used to reduce temporal coherence. However, the brightness of an LED per unit area is low, making it difficult to attain sufficient brightness if the size of the light emitting surface is reduced to ensure spatial coherence. Therefore, we focus on a projector light source that excites a yellow phosphor

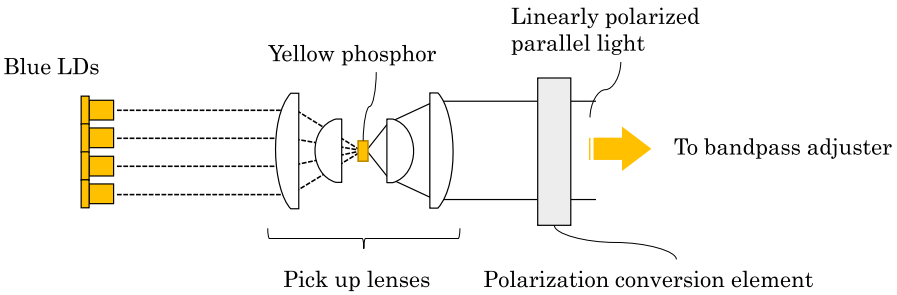

Fig. 2 Schematic diagram of yellow phosphor excitation structure in projector.

with a high-power blue LD that is temporally incoherent but has high intensity brightness in the same light-emitting area.

Figure 2 shows a schematic drawing of an optical system using a yellow phosphor as a light source in a projector. Many projectors equipped with solid-state light sources with high luminous flux have multiple high-output blue LDs as light sources, and more than half of the light is focused on one point on the yellow phosphor to excite yellow light.[18] Here, the light converted into fluorescence by the yellow phosphor of the projector has a moderately wide FWHM of about 100 nm centered on the green band and is high-power light of about several watts to several tens of watts. Thus, it should be a suitable light source for adjusting temporal coherence.

The light from the yellow phosphor is collimated and incidents the linear polarizer as parallel light. The output light is a high-power parallel light with linearly polarization. These features are important for obtaining sufficient cut-on/off characteristics in the bandwidth adjuster, which will be described in Section 3.

3 Bandwidth Control

There are various methods for trimming a desired wavelength band from wide bandwidth light using a band-pass filter. In addition to using BPF with a dielectric multilayer film, there are methods that use light dispersed by a blazed diffraction grating,[19] a diffraction grating using liquid crystal,[20] or a prism. However, with the spectroscopy method using a diffraction grating or prism, it is difficult to handle light with a wide beam width, and the device tends to be large because a certain optical path length is required. Therefore, as a high-power light source, we used a dielectric multilayer BPF to use the light emitted from the projector with a beam width of about 20 to 30 mm.

In the bandwidth adjustment section, two types of dichroic mirrors are arranged as a long pass filter (LPF) and short pass filter (SPF). A dichroic mirror with a dielectric multilayer film formed on its surface can selectively transmit or reflect a specific wavelength band by utilizing the phase difference of light that occurs when going back and forth between each layer. When constructing a BPF, the steeper the increase in the transmittance characteristic of the dichroic mirror around the cut-on/off wavelength, the more light outside the desired band can be removed. To improve this characteristic, it is necessary to understand the incident light angle characteristic and the polarization characteristic of the dichroic mirror. These are important properties to be considered in designing dielectric multilayer films.[21]

3.1 Incident Light Angle Characteristics of Dichroic Mirror

A dichroic mirror has a structure in which dielectrics with different refractive indices are formed into thin films by vapor deposition or similar processes, and films with high refractive indices and films with low refractive indices are alternately laminated. Due to this structure, the light reflected at each interface has a different phase difference, and the interference between them makes it possible to selectively reflect or transmit a specific wavelength. The light obliquely incident on each layer has a smaller phase difference than the light vertically incident. Therefore, when the angle of incident light to the dichroic mirror changes, the phase difference between the incident light and the reflected light changes accordingly, and the transmittance characteristic changes. Because the cut-on/off wavelength is generally shifted to the shorter

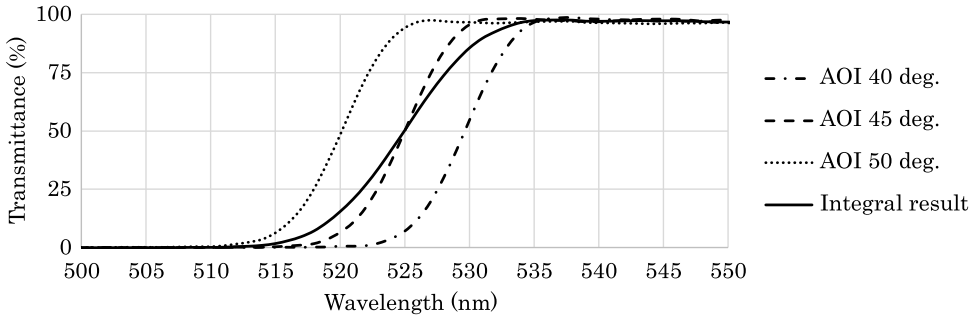

Fig. 3 Dependence of incident light angle on transmittance in a dichroic filter.

wavelength side when the light with a larger incident angle on the dichroic mirror, this phenomenon is called blue shift.[22] This is the incident light angle characteristic of the dichroic mirror.

The characteristics received when light is obliquely incident on the dichroic mirror can be obtained by calculating the convolution integral of the angular characteristics of the dichroic mirror and the normalized light distribution of incident light intensity. Figure 3 shows the wavelength characteristics of three types of light (40 deg, 45 deg, and 50 deg) with different incident angles, and it can be seen that the cut-on wavelength differs depending on the incident angles. When light with multiple incident angles is included, the solid line characteristic is obtained as the sum of their convolutions. Therefore, the parallelism of light is important for the slope-characters of the cut-on wavelength.

The parallel light whose incident light angles are only components that completely match the aforementioned angles receives the transmittance characteristics directly from the dichroic mirror. Therefore, the cut-on wavelength is the same at 525 nm for both the light distribution of the incident light with a wide angle (solid line) and that of parallel light (dashed line). However, the slope of the transmittance characteristic is steeper when the incident light is parallel light (dashed line) than in other cases. For this reason, the light incident on the dichroic mirror should ideally be close to parallel light.

In the case of oblique incidence, s-polarized light and p-polarized light can be defined by the difference in the vibration direction of the electric field with respect to the plane of incidence. The boundary conditions when light is transmitted or reflected at each boundary surface between air and multilayer films differ depending on this polarization state, so the transmittance/reflectance characteristics are shifted along the wavelength axis depending on the polarization state of the incident light. Therefore, if the light incident on the dichroic mirror contains both s- and p-polarized light, the slope characteristics become poor as described previously.

3.2 Implementation of BPF with Variable Bandwidth

The bandwidth adjuster consists of LPF and SPF with an angle adjustment mechanism using a turntable as shown in Fig. 4. By cutting short wavelength light with LPF and cutting long wavelength light with SPF, the BPF allows the light in the band between their cut-off wavelength to

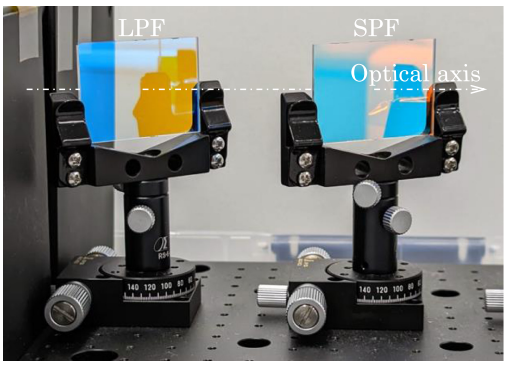

Fig. 4 Bandwidth controlling unit.

pass through. When a dichroic mirror is used as a cut filter, the more the collimation of the incident light collapses and the less linear the polarized light, the poorer the slope characteristics become due to the above-mentioned angular dependence. Therefore, it is important that the light incident on the filter is parallel and has a single linear polarization. Based on these characteristics, by passing parallel light with uniform polarization through this unit, this unit functions as a BPF with a variable transmission bandwidth and sufficient cut characteristics due to the angular dependence of each dichroic mirror.

If the rotation directions of the LPF and SPF are the same, the incident light is refracted by the thickness of each dichroic mirror, so the optical axis is unintentionally shifted. To solve this problem, the dichroic mirrors are rotated in opposite directions to cancel out the effects of optical axis deviation before and after the transmission of each dichroic mirror, thereby minimizing the amount of optical axis deviation.

Further, the cut-off wavelength of each dichroic mirror at 45 deg incidence should ideally be longer in SPF than in LPF. This is because in the BPF that combines LPF and SPF, such as that in this study, the adjustment range of the transmission wavelength band can be increased by taking into account the dependence on incident light angle. If this relationship were to be reversed, almost no light would pass through the BPF with each mirror tilted at 45 deg, and the adjustment width by rotation would be wasted.

3.3 Proposed System

Figure 5(a) shows the layout of the CGH reconstruction optical system to which the proposed light source device is applied, and the actual photograph is shown in Fig. 5(b). The proposed device is divided into a parallel light generation section, a bandwidth adjustment section, and a point light source generation section for each function. In the parallel light generation section, a commercially available 3LCD projector (EF-100W, EPSON) was modified as described in Sec. 2.3 and placed such that parallel light with high brightness could be obtained. The light source is a blue LD and yellow phosphor, and the maximum luminous flux is 2000 lm. This makes it possible to generate high-brightness parallel light that is linearly polarized. By making this light incident on the bandwidth adjustment section, a sufficient cut characteristic is obtained from the dichroic mirror. The LPF and SPF used in this device are the fluorescence dichroic filter (cut-on wavelength = 525 nm, #67-081) and the dichroic SPF (cut-off wavelength = 550 nm, #69-215) from Edmund Optics. The results of s-polarized transmittance characteristics measured using a spectrophotometer (UH4150, Hitachi) are shown in Fig. 6. When scanning spectrometers that utilize diffraction gratings or prisms, the measured slope characteristics of the filter change depending on the band width of the scanning light.[19] The line in Fig. 6 is the result of measurement with the band width of 5 nm.

After the aforementioned bandwidth adjustment unit is implemented, a point light source generation unit is arranged. An objective lens is placed in the point light source generation unit, and parallel light whose bandwidth has been adjusted is imaged at the back focal position. By arranging an aperture at this focal position, the present light source device functions as a

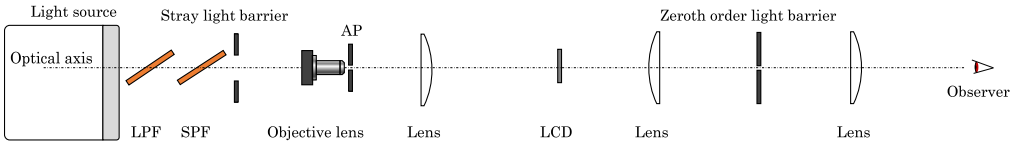

(a)

(b)

Fig. 5 (a) Proposed system layout and (b) actual appearance.

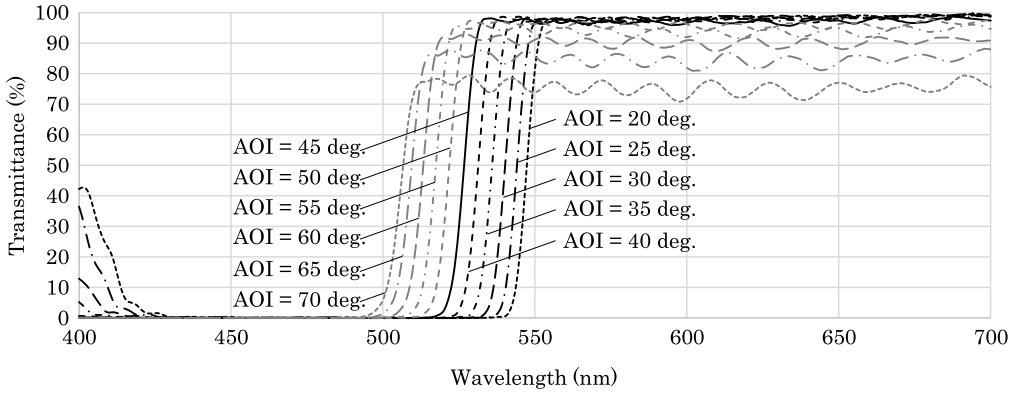

(a) LPF

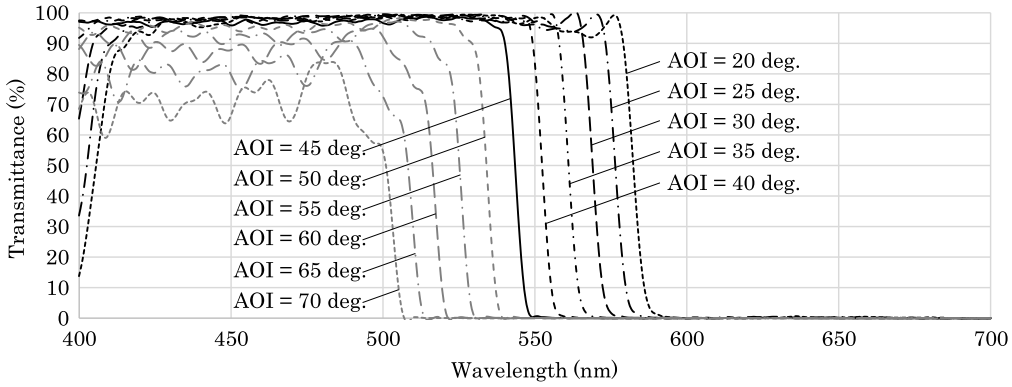

(b) SPF

Fig. 6 s-polarized angle characteristics of each dichroic mirror.

light source in which the opening of the aperture acts as a light emitting surface. The projector used here has a nominal brightness of 2000 lm, but in this device, we used an output equivalent to 1000 lm in consideration of the thermal effects of the optical parts near the condensing part, such as the objective lens and aperture.

After the developing proposed light source device, we arranged a general phase-type electro-holography reconstructing optical system. A $4f$ optical system is arranged in this reconstruction optical system, and it is possible to remove the light that hinders viewing the reconstructed image, such as the zeroth order light.[23] The light emitted from the aperture of the proposed light source device is collimated by the subsequent collimating lens and enters the LCD on which the hologram is displayed. The light diffracted by the LCD enters the $4f$ optical system together with the direct light. The direct light is condensed at the focal position of the front lens of the $4f$ optical system and blocked by the mask placed here. After that, the light is collimated again by the rear lens of the $4f$ optical system, and only the light necessary for reconstructing the holographic image reaches the observer. Such a path allows the observer to observe the band-width adjusted reconstructed image.

4 Experiment

4.1 Performance Test

The features of the proposed device are that the bandwidth can be adjusted freely and that it has high brightness because it is equipped with a high-power light source. To verify these two characteristics, we measured the spectrum on the liquid crystal panel surface and the illuminance immediately after the mask when the bandwidth was changed.

The parameters of the light source device in this experiment are shown in Table 1. For measuring illuminance and spectrum, T10A(KONICAMINOLTA) and CS2000A (KONICAMINOLTA) were used as instruments, respectively, and a standard white plate was

Table 1 Parameters of proposed system.

Light source system		
Light source (projector)		EF-100W/modified ※ 50% brightness mode
LPF	Cut-on wavelength (s-polarized light)	526.7 nm
SPF	Cut-off wavelength (s-polarized light)	543.5 nm
Objective lens	NA	0.4
	Magnification	×20
	Focal length	10 mm
Aperture size		0.1 mm × 0.1 mm

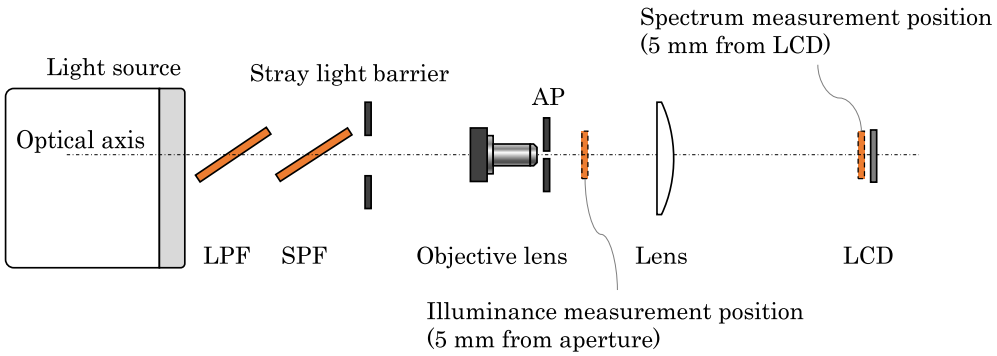

Fig. 7 Placement of the measuring instrument.

placed on the measurement surface during spectrum measurement. The measurement positions of the spectrum and illuminance are shown in Fig. 7. The target of the center wavelength (CWL) of the transmission light was adjusted to 555 nm, which is the peak of the luminous efficiency function.

Figure 8 shows the measurement results of the transmitted light spectrum when the transmission bandwidth of the BPF is changed. Here, while the FWHM changes from 60 to 6 nm, the incident light angle to the LPF and SPF gradually decrease and increase, respectively.

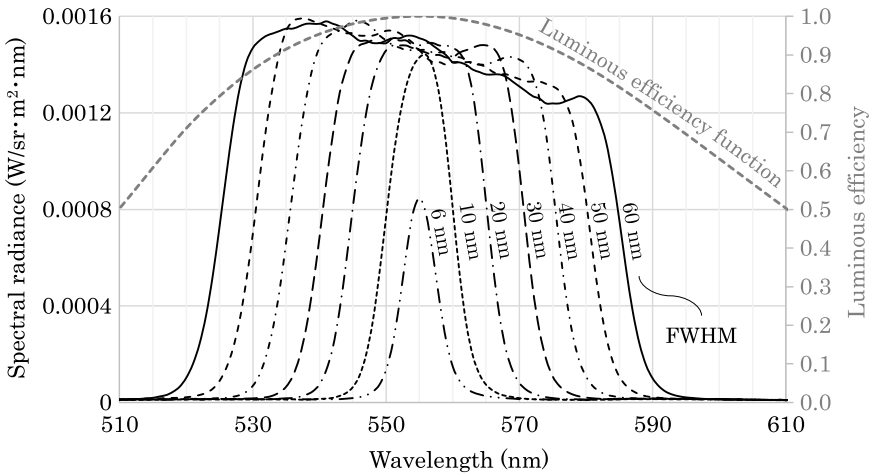

Fig. 8 Evaluation result of spectra when adjusting bandwidth.

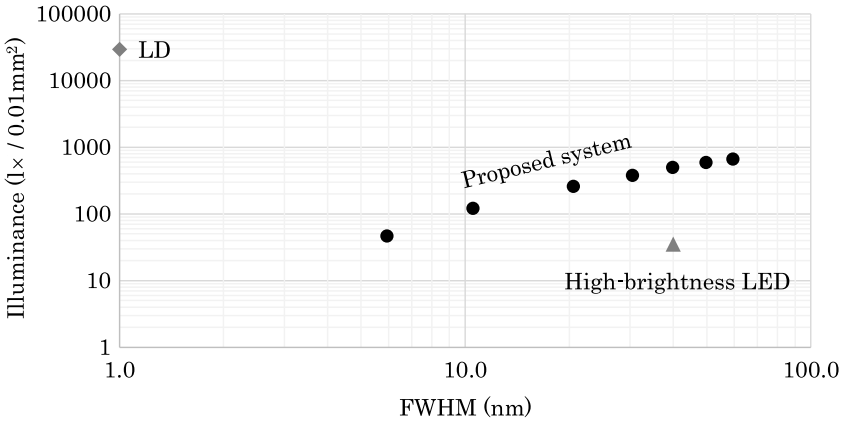

Fig. 9 Brightness of proposed system.

In the BPF with this configuration, the output light intensity greatly decreased when the FWHM fell below 6 nm, so the lower limit of the FWHM adjustment range in this system was 6 nm. Conversely, even if the incident angle to the SPF is 0 deg, the cut-off wavelength cannot be shifted further to the long wavelength side, so the upper limit of the FWHM adjustment range in this system was 60 nm. The CWL of transmitted light is 555 nm, verifying that the transmission band of the BPF can be adjusted as intended within the range from 6 to 60 nm.

The results of illuminance measurement are shown in Fig. 9, along with a green LD (532 nm) and a commercially available high-brightness green LED for reference. The illuminances of the LD and high-brightness LED shown in Fig. 9 were not actually measured but are examples of a commercially available light source. To facilitate comparison with the proposed system, the illuminances shown in the graphs are all converted values when the emission area, solid angle, and polarization state are adjusted to the measurement conditions of this study. The results in Fig. 9 demonstrate that the brightness decreases as the temporal coherence increases. This is because the integrated value of the spectrum is the emitted light energy, which can be considered an indication that the bandwidth adjustment mechanism functions correctly. Although the illuminance per 0.01 mm^2 is not as bright as that of LDs, the illuminance when FWHM is adjusted to 6 nm, which is the narrowest band, is almost equivalent to that of high-brightness LEDs. We also determined that the illuminance with a FWHM of 30 nm or more can be used as a light source that is 1 order of magnitude brighter than a high-brightness LED.

4.2 CGH Reconstruction Evaluation

Next, we reconstructed the CGH with the light whose bandwidth was adjusted using the proposed device and took pictures with the camera. The results demonstrated the relationship between the FWHM and the speckle contrast value. Images captured by camera are often used to calculate the speckle contrast. As described in Sec. 2.1, the speckle pattern depends on the light capture angle, so the camera's F-number should be adjusted to the corresponding value of the pupil diameter so the imaging optical system has an modulation transfer function (MTF) equivalent to that of the human eye.[24] Here, the pupil diameter is a parameter that changes depending on the brightness of the surrounding environment and the reconstructed image.[25] Therefore, if the speckle visible to the human eye is to be faithfully constructed, the F-number of the camera should be changed for each brightness of the environment and the reconstructed image. However, as the purpose of this study was only to determine the effect of the coherence of the light source, the F value was fixed at 7.1. This F-number is equivalent to a pupil diameter of 3.2 mm[26] when viewing images with the brightness of a typical indoor theater.[24] Using the captured image of the reconstructed image and the relational expressions of Eqs. (1)–(3), it is possible to quantitatively evaluate the relationship between the speckle intensity and the light source bandwidth from the captured image of the CGH reconstructed image.

Table 2 Parameters of CGH reconstruction evaluation.

CGH reconstruction system		
Lens	Focal length	100 mm
LCD	Resolution	1920 × 1080 px.
	Pixel pitch	7.0 um
	Type	Transmissive Thin film transistor
CGH object		
Object shape		Teapot
CGH calculation method		Point-based method
Distance from observer		450 mm
Size		9 mm

The parameters of the proposed system and CGH parameters in this experiment are shown in Table 2. In the experiment, CGHs were calculated by the point-based method.[27] In this method, the surface of the object is treated as a collection of minute point light sources, and the interference fringes formed on the hologram surface by each object light source and the reference light are calculated and recorded as a hologram. Figure 10 shows a photograph of the reconstructed images. Figure 10(a) is an input object before CGH calculation, and Figs. 10(b)–10(h) are photographs of reconstructed images when the FWHM of the light is changed from 6 to 60 nm. Speckle noise occurs in these reconstructed images, and due to the difference in temporal coherence, it can be seen that the resolution of Fig. 10(h) is lower than that of Fig. 10(b), but the speckle noise is reduced. Figure 11(a) shows a graph in which C_s is calculated by Eq. (1) using part of these images, and the relationship with each FWHM is plotted. The dashed line in Fig. 11(a) shows the theoretical curve estimated by Eq. (3) for FWHM of 30 nm. The calculation range of C_s was set to the 512 pixel square area within the frame shown in Fig. 11(b). Although the results deviate from the theoretical curve, C_s monotonically decreases with increasing FWHM. The cause of this deviation is discussed in Sec. 5.1. Thus, we determined that speckle noise can be controlled by adjusting the bandwidth of the light source and controlling the temporal coherence.

5 Discussion

5.1 Speckle Contrast

The relationship between speckle contrast and bandwidth shown in Fig. 11 deviates from that shown in Eq. (3). Specifically, according to Eq. (3), the FWHM and the speckle contrast should have an inversely proportional relationship. However, when FWHM is narrow, the calculated C_s values deviate from the theoretical curve shown by the dashed line in Fig. 11. There are two possible reasons for this. The first is that the spatial coherence is low because the size of the aperture used in this experiment is 0.1 mm × 0.1 mm. A device having a structure in which the spatial coherence can be freely adjusted would be needed to investigate further. The second reason is that the spectral shapes are different when the spectra normalized for FWHM and peak intensity are overlaid and compared for each FWHM as shown in Fig. 12. Previous studies[11,14,28] that investigated the relationship between FWHM and speckle noise often assume that the spectral shape of the light source is a Gaussian spectrum. Therefore, the FWHM used as an index of bandwidth in the proposed device may not necessarily be directly proportional to the temporal coherence. These two reasons are important factors to be considered in examining the relationship between controlled coherence and C_s and should be investigated further.

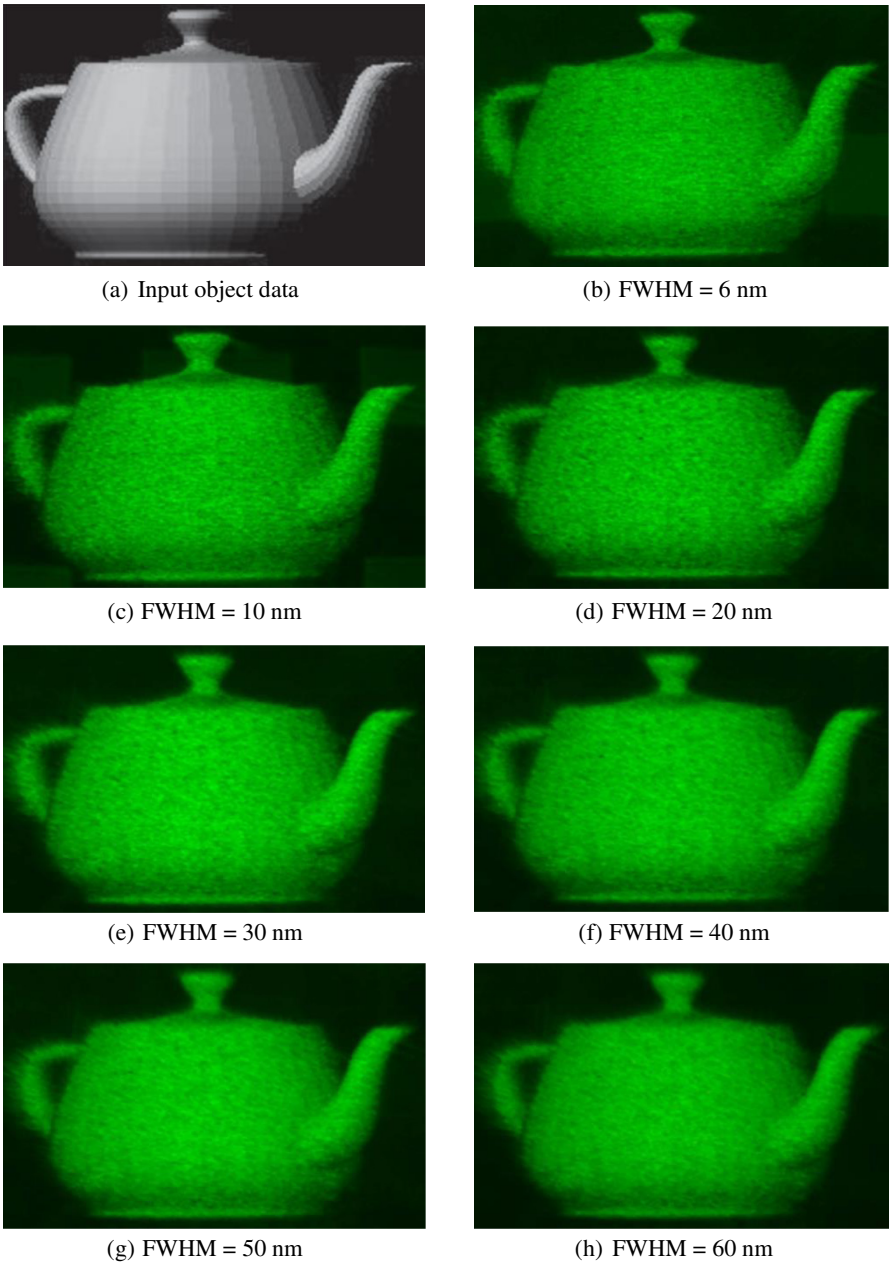

(a) Input object data (b) FWHM = 6 nm

(c) FWHM = 10 nm (d) FWHM = 20 nm

(e) FWHM = 30 nm (f) FWHM = 40 nm

(g) FWHM = 50 nm (h) FWHM = 60 nm

Fig. 10 Photograph of the reconstructed images: (a) input object data, (b) FWHM = 6 nm, (c) FWHM = 10 nm, (d) FWHM = 20 nm, (e) FWHM = 30 nm, (f) FWHM = 40 nm, (g) FWHM = 50 nm, and (h) FWHM = 60 nm.

5.2 Brightness

The brightness measurement results of our study are shown in Fig. 8. The performance of the proposed system varies greatly depending on the light source used, i.e., the brightness of the projector. The EF100W used for the light source is a projector with a nominal brightness of 2000 lm, but considering the thermal safety of the optical parts, it was used at an output of about 1000 lm, so the maximum performance value in this system can be expected to be doubled. For example, if a projector whose brightness is 10,000 lm is installed in the same way, the brightness of the system can be expected to be about 10 times that of the results measured in this study. As a result, the difference in brightness widens further, and a light source about two orders of magnitude brighter than high-brightness LEDs should be feasible. A drastic improvement in brightness should be possible with the introduction of a high-output projector after ensuring the heat resistance of the optical components.

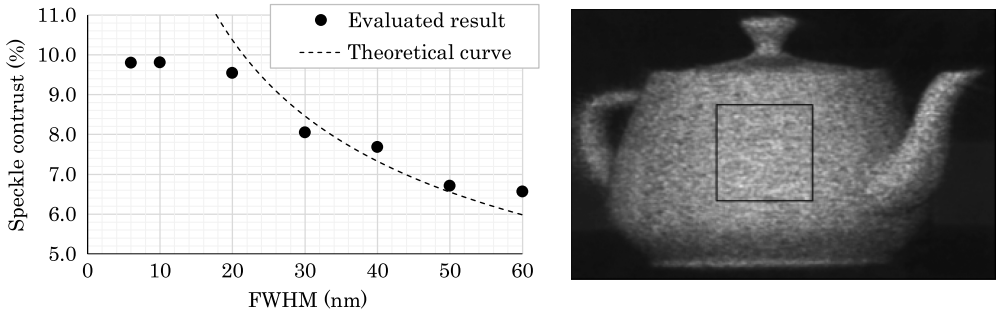

Fig. 11 Speckle contrast calculated result: (a) FWHM versus speckle contrast and (b) calculation area of the speckle contrast.

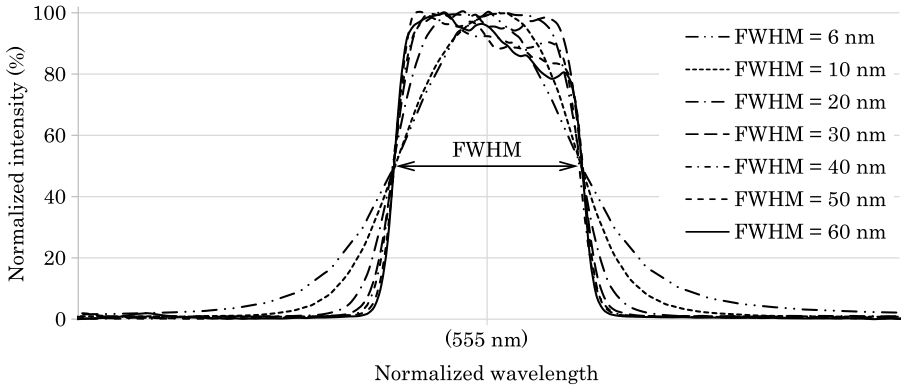

Fig. 12 Normalized spectra of light source. Vertical and horizontal axes are normalized by intensity and FWHM, respectively.

6 Conclusion

We have developed a high-power light source with adjustable temporal coherence using a yellow phosphor light source in a projector. The evaluation of the light source demonstrates that the bandwidth can be adjusted in the range of 6 to 60 nm, which enables stepless control of the temporal coherence. Furthermore, the brightness in the same light-emitting area was higher than that of commercially available high-brightness LEDs. In the CGH reconstruction experiment, we determined that the speckle noise can be controlled in the range of about 6.5% to 10% by controlling the temporal coherence. In addition, the captured images showed that the higher the temporal coherence, the higher the speckle contrast. Furthermore, the photographed image showed that the high resolution exhibited the same behavior as the speckle contrast.

From the above results, by controlling the temporal coherence of the light source using the proposed system, it is possible to search for the optimum balance between the resolution of the reconstructed image and the strength of the speckle noise. Thus, the proposed system should be useful for providing a 3D image of image quality in accordance with the subjectivity of the viewer or the purpose of the 3D image provider.

As mentioned in Sec. 5.1, the following will need to be addressed in future work: the development of a light source device with improved coherence adjustment flexibility by adding a spatial coherence adjustment mechanism, measurement of the relationship between temporal coherence and resolutions of reconstructed images, and clarification of the relationship between spectral shape of illumination light and temporal coherence. Then, subjective evaluation experiments should be conducted to investigate the optimal coherence value with respect to the situations in which CGH reconstructed images are viewed.

Data Availability

The data that support the observations of this work would be made available by the corresponding author upon reasonable request.

Acknowledgments

These research results were obtained from the commissioned research (Grant No. 06801) by the National Institute of Information and Communications Technology (NICT), Japan.

References

1. J. W. Goodman, *Speckle Phenomena in Optics: Theory and Applications*, Roberts and Company Publishers (2007).
2. Y. Sakamoto, T. Oshinomi, and K. Matsuno, "Method of calculating speckle-reduced hologram data using a convergence light wave for a computer-generated hologram," *Appl. Opt.* **62**(8), 1970–1976 (2023).
3. F. Wyrowski and O. Bryngdahl, "Iterative Fourier-transform algorithm applied to computer holography," *JOSA A* **5**(7), 1058–1065 (1988).
4. Y. Takaki and M. Yokouchi, "Speckle-free and grayscale hologram reconstruction using time-multiplexing technique," *Opt. Express* **19**(8), 7567–7579 (2011).
5. Y. Mori, T. Fukuoka, and T. Nomura, "Speckle reduction in holographic projection by random pixel separation with time multiplexing," *Appl. Opt.* **53**(35), 8182–8188 (2014).
6. B. Lee et al., "Wide-angle speckleless DMD holographic display using structured illumination with temporal multiplexing," *Opt. Lett.* **45**(8), 2148–2151 (2020).
7. M. Makowski, "Minimized speckle noise in lens-less holographic projection by pixel separation," *Opt. Express* **21**(24), 29205–29216 (2013).
8. M. N. Akram et al., "Laser speckle reduction due to spatial and angular diversity introduced by fast scanning micromirror," *Appl. Opt.* **49**(17), 3297–3304 (2010).
9. C. Graetzel, M. Suter, and M. Aschwanden, "Reducing laser speckle with electroactive polymer actuators," *Proc. SPIE* **9430**, 943004 (2015).
10. S. Kubota and J. W. Goodman, "Very efficient speckle contrast reduction realized by moving diffuser device," *Appl Opt.* **49**(23), 4385–4391 (2010).
11. T. Iwai and T. Asakura, "Speckle reduction in coherent information processing," *Proc. IEEE* **84**(5), 765–781 (1996).
12. S. Lee et al., "Light source optimization for partially coherent holographic displays with consideration of speckle contrast, resolution, and depth of field," *Sci. Rep.* **10**(1), 18832 (2020).
13. Y. Ito and Y. Sakamoto, "Method for reducing speckle contrast in electro-holography illuminated by multi-mode optical fiber," *Proc. SPIE* **12026**, 120260C (2022).
14. D. V. Kuksenkov et al., "Multiple-wavelength synthetic green laser source for speckle reduction," *Proc. SPIE* **7917**, 79170B (2011).
15. Y. Deng and D. Chu, "Coherence properties of different light sources and their effect on the image sharpness and speckle of holographic displays," *Sci. Rep.* **7**(1), 5893 (2017).
16. K. Kuroda, "Laser speckle noise," *Rev. Laser Eng.* **39**(6), 390–394 (2011).
17. G. Parry, "Speckle patterns in partially coherent light," in *Laser Speckle and Related Phenomena*, J. C. Dainty, Ed., pp. 77–121, Springer Berlin Heidelberg (1975).
18. C.-T. Yeh et al., "Luminescence material characterizations on laser-phosphor lighting techniques," *Opt. Express* **27**(5), 7226–7236 (2019).
19. M. Ziter et al., "Laser-based assessment of optical interference filters with sharp spectral edges and high optical density," *Surf. Coatings Technol.* **241**, 54–58 (2014).
20. K. A. Rutkowska and A. Kozanecka-Szmigiel, "Design of tunable holographic liquid crystalline diffraction gratings," *Sensors* **20**(23), 6789 (2020).
21. R. Pegis, "An exact design method for multilayer dielectric films," *JOSA* **51**(11), 1255–1264 (1961).
22. J. Reichman, *Handbook of Optical Filters for Fluorescence Microscopy*, Chroma Technology Corporation (2000).
23. T. Kurihara and Y. Takaki, "Improving viewing region of $4f$ optical system for holographic displays," *Opt. Express* **19**(18), 17621–17631 (2011).
24. S. Roelandt et al., "Standardized speckle measurement method matched to human speckle perception in laser projection systems," *Opt. Express* **20**(8), 8770–8783 (2012).
25. C. H. Graham, *Vision and Visual Perception*, John Wiley & Sons Inc. (1965).
26. J. Pokorny and V. Smith, "How much light reaches the retina?" in *Colour Vis. Deficiencies XIII: Proc. Thirteenth Symp. of the Int. Res. Group on Colour Vis. Deficiencies*, Pau, France, July 27–30, 1995, Springer, pp. 491–511 (1997).

27. T. Ichikawa, T. Yoneyama, and Y. Sakamoto, "CGH calculation with the ray tracing method for the fourier transform optical system," *Opt. Express* **21**(26), 32019–32031 (2013).
28. J. G. Manni and J. W. Goodman, "Versatile method for achieving 1% speckle contrast in large-venue laser projection displays using a stationary multimode optical fiber," *Opt. Express* **20**(10), 11288–11315 (2012).

Takuo Yoneyama is currently a PhD candidate at Hokkaido University, Japan. His current research interests include optical engineering and electro-holography.

Yuji Sakamoto is a professor at the Graduate School of Information Science and Technology, Hokkaido University, Japan. He has been engaged in research on computer-generated hologram, 3D image processing, and computer graphics.